Langmuir
Article
pubs.acs.org/Langmuir

Methylene Blue Incorporation into Alkanethiol SAMs on Au(111): Effect of Hydrocarbon Chain Ordering

Doris Grumelli,*[,†] Lucila P. Méndez De Leo,[‡] Cecilia Bonazzola,[‡] Vlad Zamlynny,[§] Ernesto J. Calvo,[‡] and Roberto C. Salvarezza[†]

[†]*Instituto de Investigaciones Fisicoquímicas Teóricas y Aplicadas, 1900 La Plata, Buenos Aires, Argentina,* [‡]*INQUIMAE, Departamento de Química Inorgánica, Analítica y Química Física FCEN, UBA, Ciudad Universitaria, Pabellón II, Buenos Aires, Argentina, and* [§]*Chemistry Department, Acadia University, University Avenue, Wolfville, Nova Scotia, Canada*

Received December 5, 2009. Revised Manuscript Received March 16, 2010

A detailed polarization modulation infrared reflection absorption spectroscopy, scanning tunneling microscopy, and electrochemical study on methylene blue (MB) incorporation into alkanethiolate self-assembled monolayers (SAMs) on Au(111) is reported. Results show that the amount of MB incorporated in the SAMs reaches a maximum for intermediate hydrocarbon chain lengths (C10−C12). Well-ordered SAMs of long alkanethiols (C > C12) hinder the incorporation of the MB molecules into the SAM. On the other hand, less ordered SAMs of short alkanethiols (C ≤ C6) are not efficient to retain the MB incorporated through the defects. For C12 the amount of incorporated MB increases as the SAM disorder is increased. This information is essential to the design of efficient thiol-based Au vectors for transport and delivery of molecules as well as thiol-based Au devices for molecular sensing.

Introduction

There is a great interest in the development of sensitive and specific chemical and biological systems on metallic platforms due to their potential applications in sensor, biosensor, biocatalytic devices, and drug delivery systems.[1−3] Their development needs a precise control of the metal−organic interface in different environments.

Self-assembled organic monolayers such as thiols (SAMs) have been shown to be the most promising systems to modify the surfaces of well-defined, rough, nanoparticle, nanorod, nanoshell, or nanocage gold substrates because they provide an organic platform of controllable molecular thickness able to anchor different species by nonspecific interactions or covalent bonding.[2,4−9] In particular, the use of nonspecific interactions to trap ions, molecules or biomolecules in SAM-covered gold substrates is a viable strategy for building different types of devices by the bottom-up approach.[10−12] Also nonspecific binding has been used to load hydrophobic drugs onto gold nanoparticles, allowing conjugation without structural modification of the drug payload. In this case hydrophobic pockets are created inside the monolayer of the gold nanoparticles into which hydrophobic materials can be partitioned.[13−16] However, a clear correlation between SAM ordering and nonspecific binding and delivering of molecules is still lacking understanding.

In previous papers,[17,18] we have used methylene blue (MB), a lipophilic redox molecule, as a probe to understand the nonspecific incorporation (delivery) into (from) SAMs of different thickness and terminal groups. Methylene blue (MB) on gold and thiolate-covered gold have been studied for different applications. In fact, MB incorporated to thiolate DNA covered Au has been proposed for developing MB-based sequence-specific electrochemical DNA sensors.[19] It has also been reported that methylene blue in dodecanethiol-capped gold nanoparticles exhibit electrocatalytic activity for ferricyanide reduction.[20] Methylene blue molecules adsorbed as a single layer on gold nanospheres have been proposed as one of the most promising imaging technique for gold nanoparticle-based contrast agents in tumor detection.[21] Modification of gold nanocages surfaces with dyes such as methylene blue is also important for tracers in lymph node mapping.[22] In our previous studies −COOH and $-CH_3$ terminated alkanethiols

*Corresponding author. E-mail: doris@inifta.unlp.edu.ar. Fax: 542214254642. Telephone: 54221425430.

(1) Cheng, Y.; Samia, A. C.; Meyers, J. D.; Panagopoulos, I.; Fei, B. W.; Burda, C. *J. Am. Chem. Soc.* **2008**, *130*, 10643–10647 .
(2) Cai, T. G. W.; Hong, H.; Sun, J. *Nanotechnol., Sci. Appl.* **2008**, *1*, 17–32.
(3) Wilbur, J. L.; Whitesides, G. M. In *Nanotechnology*; Timp, G., Ed.; Springer Verlag: New York, 1999.
(4) Bonanni, B.; Bizzarri, A. R.; Cannistraro, S. *J. Phys. Chem. B* **2006**, *110*, 14574–14580.
(5) Castellana, E. T.; Cremer, P. S. *Surf. Sci. Rep.* **2006**, *61*, 429–444.
(6) Gibson, J. D.; Khanal, B. P.; Zubarev, E. R. *J. Am. Chem. Soc.* **2007**, *129*, 11653–11661.
(7) Levicky, R.; Herne, T. M.; Tarlov, M. J.; Satija, S. K. *J. Am. Chem. Soc.* **1998**, *120*, 9787–9792.
(8) Love, J. C.; Estroff, L. A.; Kriebel, J. K.; Nuzzo, R. G.; Whitesides, G. M. *Chem. Rev.* **2005**, *105*, 1103–1169.
(9) Sandstrom, P.; Boncheva, M.; Akerman, B. *Langmuir* **2003**, *19*, 7537–7543.
(10) Yau, H. C. M.; Chan, H. L.; Yang, M. S. *Biosens. Bioelectron.* **2003**, *18*, 873–879.
(11) Lin, B.-Y. Y. Y.-C.; Lin, W.-C.; Lee, S.-H.; Kuo, C.-H.; Shyue, J.-J. *J. Colloid Interface Sci.* **2009**, *340*, 126–130.
(12) Rixman, M. A.; Dean, D.; Macias, C. E.; Ortiz, C. *Langmuir* **2003**, *19*, 6202–6218.
(13) Kim, C. K.; Ghosh, P.; Pagliuca, C.; Zhu, Z. J.; Menichetti, S.; Rotello, V. M. *J. Am. Chem. Soc.* **2009**, *131*, 1360.
(14) Lucarini, M.; Franchi, P.; Pedulli, G. F.; Gentilini, C.; Polizzi, S.; Pengo, P.; Scrimin, P.; Pasquato, L. *J. Am. Chem. Soc.* **2005**, *127*, 16384–16385.
(15) Lucarini, M.; Franchi, P.; Pedulli, G. F.; Pengo, P.; Scrimin, P.; Pasquato, L. *J. Am. Chem. Soc.* **2004**, *126*, 9326–9329.
(16) Kim, C.-k.; Ghosh, P.; Rotello, V. M. *Nanoscale* **2009**, *1*, 61–67.
(17) Tognalli, N. G.; Fainstein, A.; Vericat, C.; Vela, M. E.; Salvarezza, R. C. *J. Phys. Chem. B* **2006**, *110*, 354–360.
(18) Tognalli, N. G.; Fainstein, A.; Vericat, C.; Vela, M. E.; Salvarezza, R. C. *J. Phys. Chem. C* **2008**, *112*, 3741–3746.
(19) Pan, D.; Zuo, X. L.; Wan, Y.; Wang, L. H.; Zhang, J.; Song, S. P.; Fan, C. H. *Sensors* **2007**, *7*, 2671–2680.
(20) Liu, S. F.; Wang, L.; Zhao, F. *J. Electroanal. Chem.* **2007**, *602*(1), 55–60.
(21) Laurent, G.; Felidj, N.; Truong, S. L.; Aubard, J.; Levi, G.; Krenn, J. R.; Hohenau, A.; Leitner, A.; Aussenegg, F. R. *Nano Lett.* **2005**, *5*, 253–258.
(22) Song, K. H.; Kim, C. H.; Cobley, C. M.; Xia, Y. N.; Wang, L. V. *Nano Lett.* **2009**, *9*, 183–188.

SAMs were self-assembled on high-area nanostructured Au, a fractal substrate that exhibits surface enhanced raman spectroscopy (SERS) activity.[17,18] SERS allows a precise determination of the amount of MB incorporated and delivered to/from the SAMs. It has been found that $-CH_3$ terminated SAMs incorporated MB mainly through defects in the monolayer without a clear correlation between incorporation and the hydrocarbon chain length. Delivery of the incorporated molecules under concentration gradients or electrochemically induced molecular changes was also observed.[18] However, in our previous papers, the highly disordered surface of the SERS-active nanostructured Au should induce strong disorder in the hydrocarbon chains. Therefore, no clear correlation between hydrocarbon chain order and MB incorporation in the SAMs could be derived from our previous work.

In the present work, we studied MB incorporation into methyl-terminated alkanethiolate SAMs on smooth Au surfaces that allow us to correlate the amount of incorporated MB and SAM ordering. In fact, in this work we have used polycrystalline Au substrates with preferred (111) orientation that exhibit atomically smooth (111) terraces where molecular resolution can be achieved by STM. The degree of order in the SAMs has been varied by changing the hydrocarbon chain length, and it has been tested by using PMIRRAS. On the other hand, the amount of incorporated MB has been measured by electrochemical techniques and by PMIRRAS. Results show that the amount of MB incorporated in the SAMs reaches a maximum for intermediate hydrocarbon chain lengths (C10−C12). Well-ordered SAMs of long alkanethiols (C > C12) hinder the incorporation of the MB molecules into the SAM. On the other hand, less ordered SAMs of short alkanethiols (C ≤ C6) are not efficient to retain the MB incorporated through the defects. This information is essential to design of efficient thiol-based Au vectors for transport and delivery of molecules as well as thiol-based Au devices for molecular sensing.

Experimental Section

Gold Substrates and Chemicals. Gold evaporated on glass substrates were purchased from Arrandees, consisting of vapor deposited gold films (250 ± 50 nm in thickness) on a thin layer of chromium supported on glass slides. These polycrystalline substrates exhibit large grains after flame annealing with atomically smooth terraces separated by steps of monatomic height. The alkanethiols 1-butanethiol 99% (C4), 1-hexanethiol ≥95% (C6), 1-decanethiol 96% (C10), 1-dodecanethiol ≥98% (C12), 1-hexadecanethiol 98% (C16) and 1-octadecanethiol 98% (C18) were used as received (Aldrich Chemical Co. Milwaukee, WI). Absolute ethanol, carbon tetrachloride, and Milli-Q water were used as solvents.

Self-Assembly of Alkanethiols on Gold. The self-assembled alkanethiol monolayers (SAMs) were prepared by immersing the gold substrate into a freshly prepared 100 μM alkanethiol in absolute ethanol for 24 h at room temperature in the absence of light. Final rinsing was done with ethanol before drying under N_2.

Methylene Blue Incorporation. Methylene blue (MB) incorporation into the alkanethiolate SAMs on Au (111) was done by immersing the SAM-covered substrate into 0.03 M aqueous solution of MB for 24 h at room temperature in the absence of light. Note that we have used a longer immersion time and a larger MB concentration than those used in our previous works[17,18] in order to improve the IR signals. Afterward, the samples were rinsed with water and dried under N_2.

Characterization of Alkanethiol SAMs. The alkanethiolate SAMs, with and without MB molecules, were characterized by PMIRRAS, STM, and electrochemical techniques.

IR Experiments. Polarization modulation infrared reflection absorption spectroscopy (PMIRRAS) experiments were performed at the University of Buenos Aires, on a Thermo Nicolet 8700 (Nicolet, Madison, WI) spectrometer equipped with a custom-made external tabletop optical mount, a MCT-A detector (Nicolet), a photoelastic modulator, PEM (PM-90 with II/Zs50 ZnSe 50 kHz optical head, Hinds Instrument, Hillsboro, OR), and syncronous sampling demodulator, SSD, (GWC Instruments, Madison, WI).

The IR spectra were acquired with the PEM set for a half wave retardation at 2900 cm^{-1} for the CH stretching region and at 1500 cm^{-1} for the CH bending and aromatic region. The angle of incidence was set at 80°, which gives the maximum of mean square electric field strength for the air/gold interface. The demodulation technique developed by Corn[23,24] was used in this work. The signal was corrected by the PEM response using a method described by Frey et al.[25] Typically 8000 and 1500 scans were performed and the resolution was set for 2 and 4 cm^{-1}, respectively.

Transmission spectra for crystalline alkanethiols were measured using KBr pellets. On the other hand, transmission spectra for the liquid alkanethiols were performed in CCl_4 using a thin optical pass liquid cell with CaF_2 windows. In both cases the resolution was set to 2 cm^{-1} and 200 scans were performed.

Determination of Molecular Orientation of the SAMs. The orientation of the chains was determined using the "relative" method approach.[26,27] It relies on the availability of at least two absorption modes that correspond to differently oriented transition dipoles. In this case the CH_2 and CH_3 absorption bands were used. Briefly, in the alkanethiol SAMs the CH_3 has a relatively free rotation and is quite mobile, so it can be assumed to have no preferential orientation, i.e., $\cos^2 \Theta_{CH_3} = {}^1/_3$, while the average tilt angle of CH_2 dipoles depends on the chain orientation. During the transmittance experiments of alkanethiolate dispersions either using KBr pellet or liquid CCl_4 solution, both CH_2 and CH_3 are randomly oriented. Relative differences in the IR peak intensities for CH_2 with respect to CH_3 stretching modes between the alkanethiol SAM adsorbed at the metal surface and the randomly distributed dispersions can be attributed to a preferred orientation for the alkane chain in the SAMs on metal surface. The relationship between the areas of these peaks can be written as

$$\frac{A^R_{CH_2}}{A^R_{CH_3}} = \frac{A^T_{CH_2}}{A^T_{CH_3}} \frac{\cos^2 \Theta^R_{CH_2}}{1/3} \tag{1}$$

where A^R is the integrated intensity of a mode in the SAM measured using reflection absorption spectroscopy (RAS), A^T is the area determined using transmittance experiments on a randomly distributed sample, and Θ is the angle between the CH_2 transition dipoles and the surface normal.

The main source of errors in this method is associated with the area determination. In our estimation how such errors affect the final result (i.e., tilt angle) we assumed that the relative standard deviations (RSD_{RAS}) for areas determined in RAS experiments were 5% and the RSD for the Transmittance experiments were assumed to be much smaller and thus could be neglected. Following the propagation of error eq 2 (see Supporting Information) we found that the relative method is expected to yield reasonable errors of ±10° or less within variations of the tilt angle between 10 and 80 degrees.

$$\sigma\Theta = \frac{1}{2}\left[\left(\frac{RSD_{RAS}}{\cos^2 \Theta}\right)^2 + (RSD_{RAS})^2\right]^{1/2} \cot \Theta \tag{2}$$

STM Measurements. Scanning tunneling microscopy (STM) images were obtained using a Nanoscope IIIa microscope from

(23) Barner, B. J.; Green, M. J.; Saez, E. I.; Corn, R. M. *Anal. Chem.* **1991**, *63*, 55–60.
(24) Green, M. J.; Barner, B. J.; Corn, R. M. *Rev. Sci. Instrum.* **1991**, *62*, 1426–1430.
(25) Frey, B. L.; Corn, R. M.; Weibel, S. C. *Handbook of Vibrational Spectroscopy*: John Wiley & sons: New York, 2001.
(26) Arnold, R.; Terfort, A.; Woll, C. *Langmuir* **2001**, *17*, 4980–4989.
(27) Debe, M. K. *J. Appl. Phys.* **1984**, *55*, 3354–3366.

Veeco Instruments (Santa Barbara, CA). Commercial Pt−Ir tips were used. Typical tunneling currents and bias voltages for imaging dodecanethiol (C12) and methylene blue (MB) in C12 on Au(111) were 300 pA and 800−1000 mV, respectively.

Electrochemical Experiments. Cyclic voltammetry was performed with a potentiostat under computer control for data acquisition. The gold substrates were mounted in a conventional three-electrode cell. Solutions were purged with nitrogen. All potentials were measured and reported with respect to a Ag/AgCl (saturated KCl) reference electrode. Solutions of 0.1 M NaOH were prepared using deionized H_2O from a Milli-Q purification system (Millipore Products, Bedford).

The Au sample with MB incorporated in the SAMs was cycled in deaerated aqueous 0.1 M NaOH solution between −0.1 to −0.8 at 0.5 V s^{-1}, and the redox couple related to oxidized (MB^+), and reduced (MBH) was recorded. The charge measured from the integration of the anodic peak of the first cycle was taken as a measure of the amount of the electrochemically active MB incorporated in the SAMs.

Reductive electrodesorption of thiols from the Au substrates, with and without incorporated MB, were performed by scanning the potential from −0.2 to −1.7 at 0.05 V s^{-1} in deaerated 0.1 M NaOH aqueous solution, at room temperature. The charge density and the peak potential involved in the reductive desorption process were taken as an indication of the surface coverage by the SAM (a thiol SAM in $\sqrt{3} \times \sqrt{3}$ R30° or $c(4 \times 2)$ involves 75 μC cm^{-2}) and of the SAM stability, respectively.

Average data shown in the paper correspond to four or more samples. The error bars were calculated from the standard deviation of these data.

Results and Discussion

In Figure 1a typical STM image of a C12 SAM on the preferentially oriented (111) substrate is shown. The image shows well-defined terraces separated by mono- and diatomic steps in height with dark regions corresponding to vacancy islands produced during thiol adsorption.[28] The inset in Figure 1a shows a region of the terrace imaged at a high resolution were the $\sqrt{3} \times \sqrt{3}$ R30° lattice can be clearly observed as an ordered array of small bright spots (Inset, yellow arrow). Each bright spot corresponds to the position of a C12 molecule separated from the nearest neighbors by 0.5 nm. Note that around the vacancy island (Inset, white arrow) molecular disorder is clearly observed as the bright spots do not follow the ordered array. The disorder is more important for short alkanethiol SAMs.[27] In fact, C3 and C4 SAMs exhibit a large number of defects such as missing rows[28] or completely disordered regions coexisting with ordered domains.[29] For $n > 12$ the alkanethiol SAMs are difficult to observe by STM due to the hindered tunneling through the long hydrocarbon chains.

PMIRRAS spectroscopy was used to characterize order, orientation and packing of the SAMs of the different chain length. Figure 2 shows typical PMIRRAS spectra for C6 (Figure 2a), C12 (Figure 2b), and C18 (Figure 2c) in the CH stretching region (3000−2700 cm^{-1}). Similar spectra and band assignment have been reported[30−34] and are used here to compare with our spectra. The band at 2965 cm^{-1} is assigned to the CH_3 asymmetric stretching mode (ν_a CH_3), while the band at 2879 cm^{-1} is assigned to the CH_3 symmetric modes (ν_s CH_3). The band at 2920 and 2850 cm^{-1} are assigned to ν_a and ν_s CH_2 modes, respectively. The band at 2935 cm^{-1} is assigned to a Fermi resonance (FR) which is the combinational band of the CH_2 symmetric stretching vibration at 2850 cm^{-1} and the second harmonic of CH_2 bending vibration at 1467 cm^{-1}.[35,36] Previous IR studies[37−39] have shown that

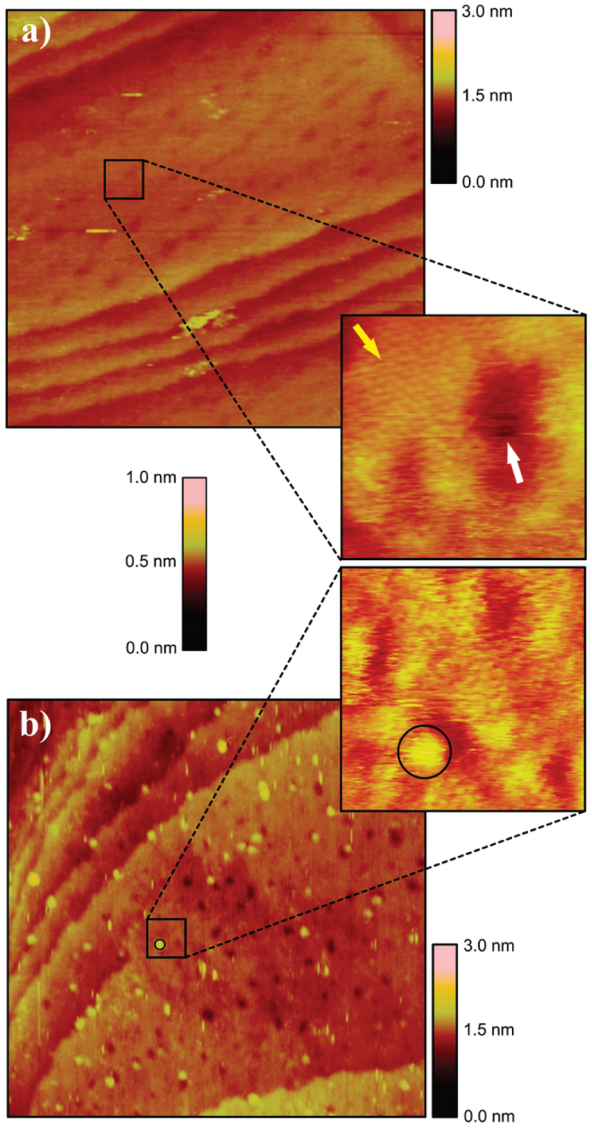

Figure 1. (a) 100 × 100 nm STM images of C12 on Au(111). Inset: 10 nm zoomed region showing the $\sqrt{3} \times \sqrt{3}$ R30° surface structure (yellow arrow) and dark regions corresponding to vacancy islands produced during thiol adsorption (white arrow). b) 100 × 100 nm STM images of MB in C12 on Au(111). Bright spots correspond to the MB molecule located in the large terraces and in the steps edges Inset: 10 nm zoomed region showing isolated domains of the C12 molecules close to the MB bright spots. The scan direction in parts a and b is top to bottom with the fast scan in the x direction. Tunneling current: 300 pA. Bias voltage: 900 mV.

(28) Vericat, C.; Vela, M. E.; Salvarezza, R. C. *Phys. Chem. Chem. Phys.* **2005**, *7*, 3258–3268.
(29) Arce, F. T.; Vela, M. E.; Salvarezza, R. C.; Arvia, A. J. *J. Chem. Phys.* **1998**, *109*, 5703–5706.
(30) Allara, D. L.; Nuzzo, R. G. *Langmuir* **1985**, *1*, 52–66.
(31) Allara, D. L.; Swalen, J. D. *J. Phys. Chem.* **1982**, *86*, 2700–2704.
(32) H. M. e. l. Finklea, J. A. *Spectroscopy* **1986**, *I*(4), 47–48.
(33) Rabolt, J. F.; Burns, F. C.; Schlotter, N. E.; Swalen, J. D. *J. Chem. Phys.* **1983**, *78*, 946–952.
(34) Snyder, R. G.; Hsu, S. L.; Krimm, S. *Spectrochim. Acta, Part A: Mol. Biomol. Spectrosc.* **1978**, *34*, 395–406.
(35) Flach, C. R.; Gericke, A.; Mendelsohn, R. *J. Phys. Chem. B* **1997**, *101*, 58–65.
(36) Snyder, R. G.; Liang, G. L.; Strauss, H. L.; Mendelsohn, R. *Biophys. J.* **1996**, *71*, 3186–3198.
(37) Porter, M. D.; Bright, T. B.; Allara, D. L.; Chidsey, C. E. D. *J. Am. Chem. Soc.* **1987**, *109*, 3559–3568.
(38) Snyder, R. G.; Maroncelli, M.; Strauss, H. L.; Hallmark, V. M. *J. Phys. Chem.* **1986**, *90*, 5623–5630.
(39) Snyder, R. G.; Strauss, H. L.; Elliger, C. A. *J. Phys. Chem.* **1982**, *86*, 5145–5150.

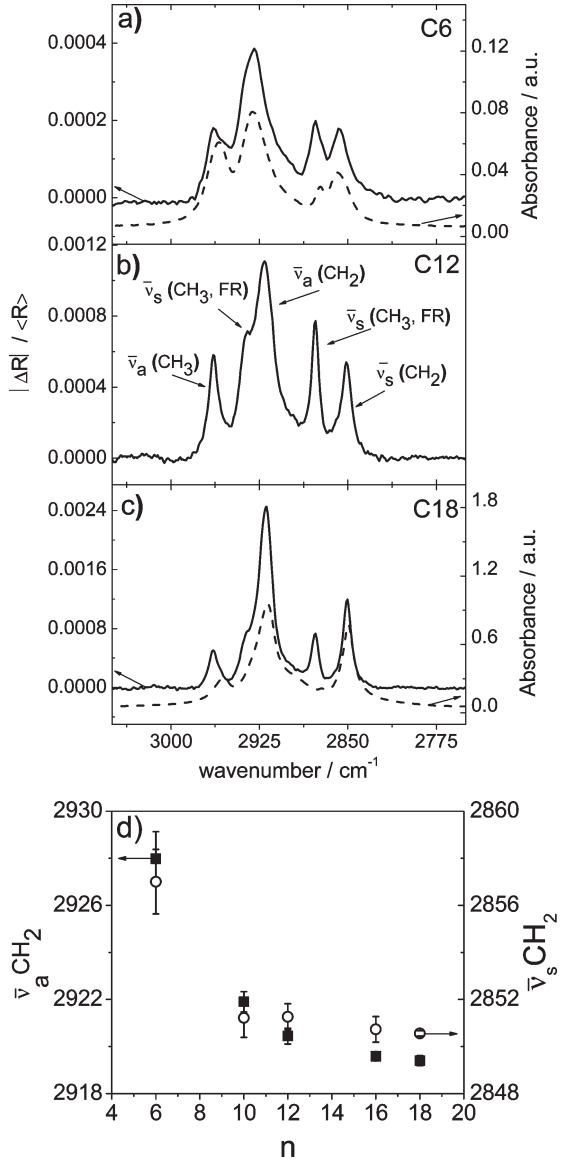

Figure 2. (-)PMIRRAS spectra of self-assembled monolayers of (a) C6, (b) C12, and (c) C18 on Au(111). Resolution was set to 2 cm^{-1} and 8000 scans were performed. (---) Transmission FTIR spectra of C6 in CCl_4 and C18 in KBr pellet. Resolution was set to 2 cm^{-1} and 200 scans were performed. (d) (■) ν_a CH_2 and (○) ν_s CH_2 position vs chain length for C6, C10, C12, C16, and C18 SAMs.

the peak position corresponding to ν_a CH_2 stretching mode can be used to assess the degree of order of alkanethiol SAMs on Au and Ag. Also, the ν_s CH_2 peak, less affected by Fermi resonance band, gives a good correlation between band positions and hydrocarbon chain order. Furthermore, it has been found that there is 8 cm^{-1} shift between the positions of infrared bands of crystalline polymethylene chains and the polymer chains in the liquid state. Porter et al.[37] have shown that SAMs of short alkanethiols ($n < 9$) have a similar behavior to that of the bulk disordered liquid phase due to the large number of defects, while SAMs of long alkanethiols ($15 \leq n \leq 21$) approach the behavior of crystalline systems.

Transmission IR spectra for a crystalline alkanethiol (C18 in a pellet KBr) and a liquid alkanethiol (C6 in a CCl_4 using a liquid cell) are shown in Figure 2 (dashed lines in Figure 2, parts a and c). In our case the peak position for ν_a CH_2 mode for crystalline C18, and a liquid C6 are observed at 2919 cm^{-1} and 2927 cm^{-1} respectively, in agreement with the 8 cm^{-1} shift already reported.[37] Therefore, the shift of the ν_a CH_2 and ν_s CH_2 bands as the hydrocarbon chain in the SAM is increased from C18 to C6 (Figure 2d) indicates a change from a crystalline ordered SAM to a less ordered SAM.

MB Characterization. Figure 1b shows a typical STM image obtained after the C12 SAM on Au(111) has been immersed in the MB containing solution. Isolated bright spots 1.4−2 nm in size can be clearly resolved in the large terraces containing the vacancy island regions (dark zones in Figure 1b). Domains of the C12 molecules can also be observed close to the bright spots (inset in Figure 1b). Following ref 40, we assign the bright spots to the MB molecules immobilized in the C12 SAM. The density of the bright spots in these images is $\approx 2 \times 10^{12}$ cm^{-2}. A detailed analysis of the bright spots locations reveals that they decorate borders of the vacancy islands and also step edges (Figure 1b). It should be noted that in both places chain disorder is expected. In fact, preferential nucleation of Ag electrodeposits has been observed by in situ STM at step edges of alkanethiolate SAMs indicating that these regions are defective sites of the monolayer[41] (see also STM images in the Supporting Information). Besides high mobility of alkanethiol molecules has been observed at step edges,[42] a fact that would favor MB incorporation at these sites. On the other hand, as mentioned above, disorder at borders of vacancy islands is evident in Figure 1a (inset). It is also evident that the isolated aromatic molecules show an enhancement in the molecular conductivity compared to neighboring alkanethiols, thus explaining the high-contrast in the STM images.[43] The smallest size of the bright spots (1.4 nm) is compatible with the size of the isolated MB molecules where the larger ones can be related to regions where several molecules of MB are incorporated into the C12 SAM.

Figure 3 shows the complete transmission (3500−1100 cm^{-1}) FTIR spectrum for MB. In addition, parts b and c of Figure 3 show zoomed regions (1700−1100, 3600−2600 cm^{-1}) where the band assignment is presented, based on previously reported data.[44] In the next part, we have indicated the bond responsible of the IR absorption by the symbol (−) between atoms. As already reported the most intense band corresponds to the vibration of the heterocyclic skeleton (ν_{hc} C−C) at 1600 cm^{-1}, which also has other minor bands at 1250−1222 cm^{-1} (Figure 3b). The C−H asymmetric and symmetric bending vibrations (δ_a C−H_3, δ_s C−H_3) appear at 1445 and 1397 cm^{-1}respectively, while the vibrations of the C−N terminal saturated dimethylamino groups are located at 1356−1340 cm^{-1}. In the 3100−2600 cm^{-1} region (Figure 3c), the bands are weaker but vibrations of the C−H groups (ν_{hc} C−H), typical of the heterocyclic compound, can be identified at 3045 cm^{-1}, as well as asymmetric and symmetric stretching vibrations (ν_a C−H_3,ν_s C−H_3) of the C−H_3 bonds in the dimethylamino groups at 2929 and 2891 cm^{-1}, respectively, and an absorption band at 2708 cm^{-1} probably related to vibrations of the $N(CH_3)_2$ terminal saturated dimethylamino groups ((ν N−$(CH_3)_2$).

(40) Vela, M. E.; Vericat, C.; Millone, M. A. D.; Fonticelli, M.; Benitez, G.; Salvarezza, R. C.; Tognalli, N. G.; Fainstein, A. *J. Nanosci. Nanotechnol.* **2006**, *6*, 2362–2367.
(41) Hagenstrom, H.; Esplandiu, M. J.; Kolb, D. M. *Langmuir* **2001**, *17*, 839–848.
(42) Stranick, S. J.; Kamna, M. M.; Krom, K. R.; Parikh, A. N.; Allara, D. L.; Weiss, P. S. *J. Vac. Sci. Technol. B* **1994**, *12*, 2004–2007.
(43) Cygan, M. T.; Dunbar, T. D.; Arnold, J. J.; Bumm, L. A.; Shedlock, N. F.; Burgin, T. P.; Jones, L.; Allara, D. L.; Tour, J. M.; Weiss, P. S. *J. Am. Chem. Soc.* **1998**, *120*, 2721–2732.
(44) Ovchinnikov, O. V.; Chernykh, S. V.; Smirnov, M. S.; Alpatova, D. V.; Vorob'eva, R. P.; Latyshev, A. N.; Evlev, A. B.; Utekhin, A. N.; Lukin, A. N. *J. Appl. Spectrosc.* **2007**, *74*, 809–816.

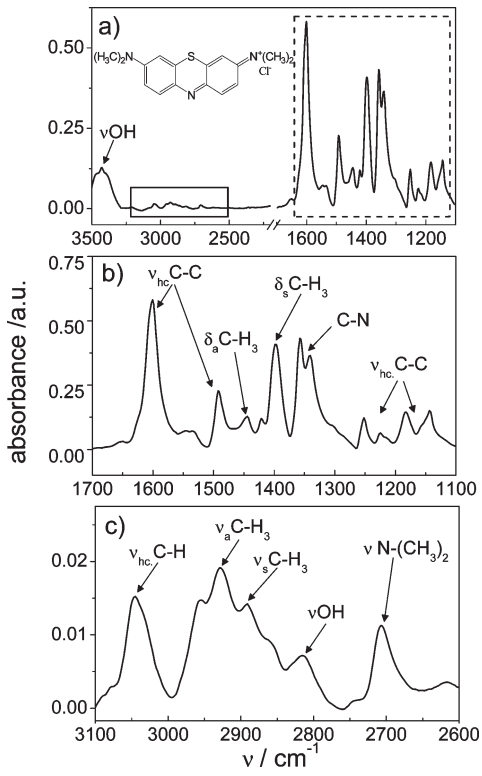

Figure 3. Transmission FTIR MB spectra (in a KBr pellet) measured with 2 cm^{-1} resolution and 200 scans. (a) FTIR spectra in the 3500- 1100 cm^{-1} region. The solid and dash line square shows the range at the zoom in parts b and c, respectively. Inset: MB chemical structure. (b) Zoom of 1700−1000 cm^{-1} MB region (solid line square in part a) with the respective assignment. (c) Zoom of 3100−2600 cm^{-1} MB region (dashed line square in part a) with the band assignment.

The two absorption bands at 2810 cm^{-1} (Figure 3c) and 3435 cm^{-1} (Figure 3a) can be related to vibrations of the OH groups forming hydrogen bonds: O−H···N and O−H···O respectively. In fact, previous IR studies[44] have shown that MB is a hydrated compound that can form hydrogen bridges of the O−H···O type with the nitrogen and atoms.

Now, we focus on the immobilized MB onto the SAM-covered Au(111) samples. Considering that submonolayer amounts of MB are expected in the alkanethiol monolayers, the most intense band at 1600 cm^{-1} region was used to test the presence of MB in the SAMs. Figure 4a shows PMIRRAS spectra recorded for C6 and C18 SAMs after immersion in the MB containing solutions followed by careful rinsing. All samples exhibit the characteristic band at 1600 cm^{-1}. Since this band corresponds to the vibration of the heterocyclic skeleton (vide infra) it can be concluded that the MB aromatic ring is far from being flat on the surface.

This result contrasts to that reported for MB on Au(111) where the molecules adsorb in the double layer region forming a $c(5 \times 5\sqrt{3})$ *rect* structure in a flat lying configuration.[45] Therefore, we conclude that the IR signal at 1600 cm^{-1} arises from molecules incorporated inside the monolayer without a free contact with the Au surface because in that case transition dipoles should be parallel to the surface and IR inactive.

In order to estimate the amount of MB wired to Au, surface electrochemical techniques were used. Figure 4b shows the cyclic voltamperometry of C6 and C18 SAM-covered Au(111) substrates after immersion in the MB containing solution. In both

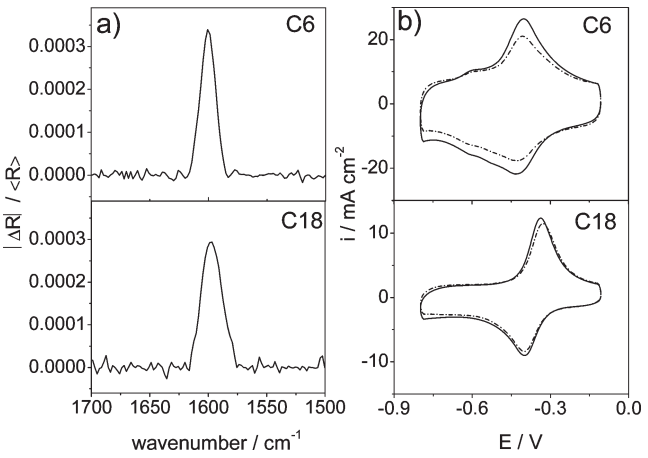

Figure 4. (a) PMIRRAS spectra (1700−1500 cm^{-1}) of MB in C6 and C18 SAMs on Au(111). Resolution: 4 cm^{-1}, 1500 scans. (b) Cyclic voltammetry of MB in SAMs of C6 and C18 (−) first cycle and (---) 12th cycle). Scan from −0.1 to −0.8 at 0.5 $V \cdot s^{-1}$ in 0.1 M NaOH aqueous solution.

cases the typical redox couples corresponding to MB^+/MBH species are clearly visible. These results confirm that the MB molecules are incorporated in the alkanethiolate SAMs and that they, or at least some of them, are electrochemically active; i.e., they are within close proximity to the Au electrode, allowing the tunneling effect to occur. Another interesting feature is that the MB molecules in the C6 SAM exhibit a more reversible behavior than those incorporated into C18 SAM (Figure 4b). In this last case, the oxidation of the MBH species to MB^+ could be more difficult because it involves the migration of anions from the electrolyte through a ordered crystalline SAM to compensate the positive charges created close to the SAM/Au interface.

After repetitive cycling the samples in the 0.1 M NaOH solution (12 cycles) a decrease in the amount of electrochemically active MB is evident for C6 while no significant changes are observed for MB incorporated into the C18 SAM (Figure 4b dashed lines). This result agrees with those reported for MB incorporated in nanostructured Au obtained from "in situ" SERS measurements at open circuit conditions.[18] In this case incorporated MB molecules were slowly released from the SAM when the Au substrate is placed in contact with a clean electrolyte. Alkanethiol SAMs on nanostructured gold with typically 8−20 nm grains in size are expected to exhibit a strong chain disorder. Therefore, one can conclude that MB incorporation is a reversible process in disordered SAMs (C6) while it is an irreversible process in highly crystalline SAMs (C18). It is interesting to note that simple adsorption of MB at the terminal methyl group can not explain the chain length dependent behavior observed for the MB release.

Using the anodic charge obtained from the first cycle of the cyclic voltammetry of the MB redox couple immobilized into the SAMs it is possible to calculate the amount of MB electrically connected to the electrode for different SAMs. Figure 5 shows the amount of wired MB (estimated from the anodic charge in the voltammograms) as a function of the number of carbon atoms (n) in the alkanethiol SAM (n = 4, 6, 10, 12, 16, 18). The plot exhibits a maximum for C12. We interpret this behavior as a result of two opposite effects. The longer hydrocarbon chain length furnishes efficient trapping of the lipophilic cation MB. However, it hinders molecule incorporation to the SAMs by making the SAM more crystalline, i.e., reducing the number of incorporation pathways.

(45) Song, Y.; Wang, L. *Microsc. Res. Tech.* **2008**, *72*, 79–84.

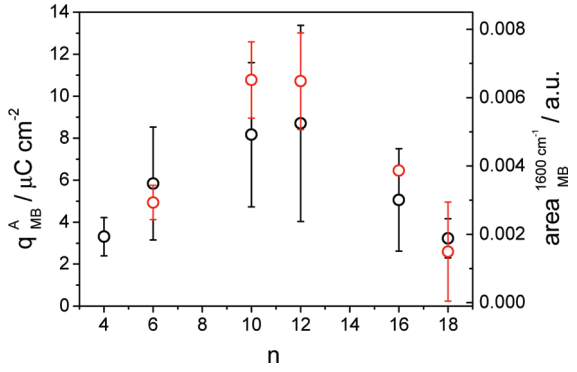

Figure 5. Black circle: anodic charge for MB (q_A^{MB}) vs the number of carbon atoms in the alkanethiol (n). Anodic charge was determined by integration of the anodic peak of the first cycle in the cyclic voltammperometry of MB in 0.1 M NaOH recorded between −0.1 and −0.8 V at 0.5 V·s^{-1}. Average and the standard deviations were taken over six or more different electrodes. Red circle: area of PMIRRAS peak at 1600 cm^{-1} for SAMs containing MB vs the number of the carbon atoms in the alkanethiol (n). The area was determined after correction of the experimental PMIRRAS spectra with the spline baseline. The symbol represented the average of four or more measurements while error bars are standard deviation .The relative standard deviations (RSD_{RAS}) for areas determined in RAS experiments were 5%.

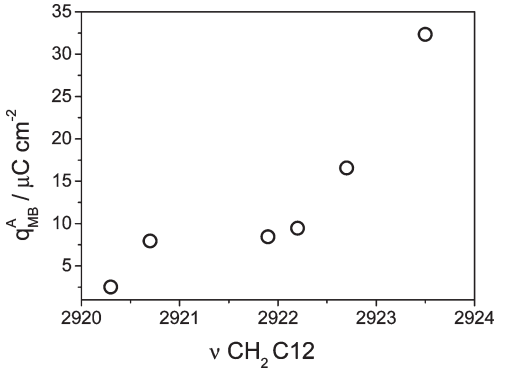

Figure 6. Anodic charge for MB vs ν_a CH_2 for different ordered C12 SAMs. The anodic charge was calculated from the CV of MB in 0.1 NaOH aqueous solution as described in the Experimental Section.

This trend is also confirmed by estimating the relative amount of MB incorporated in the different SAMs using the intensity of the 1600 cm^{-1} band as is shown in Figure 5.

Note that the results shown in Figure 5 are not consistent with simple MB adsorption on the terminal methyl group of the SAMs. In fact, longer alkanethiols have more ordered SAMs so that a higher density of methyl groups should be exposed for MB adsorption. However, in this case we expect an increase in the amount of MB with n, a fact not consistent with the PMIRRAS data showing a maximum at C10−C12. Also the maximum amount of MB at C10−C12 allows us to discard a simple model where MB molecules are adsorbed at SAM defects in direct contact with the Au surface. In fact, it is well-known that the amount of defects at SAMs decreases as the hydrocarbon chain length is increased, as revealed by capacitance measurements.[46] Therefore, if MB molecules were placed at defective sites in direct contact with the Au surface we expect a decrease in the q_A^{MB} with n rather than a plot with a maximum at C12. Therefore, results in Figure 5 indicate a more complex behavior where the degree of SAM disorder is important to incorporate the molecule, but the hydrocarbon chain−MB interactions play also an important role to retain the molecules embedded in the SAM. Note, however that we can not completely discard the presence of some MB molecules in close contact to the Au surface, in particular for SAMs of short alkanethiols where molecular defects such as missing rows have been reported.[27]

Concerning the possible paths for MB incorporation, we propose that this process takes places at disordered SAM regions such as domain boundaries, molecular vacancies, adsorbed impurities, missing rows, and step edges and around vacancy islands, where an increased chain disorder is expected. In fact, for a given alkanethiol (n constant), the quantity of MB wired to the Au substrate depends strongly on the order/disorder of the SAM. Figure 6 shows the amount of MB in different C12 SAMs as a function of the of ν_a CH_2 peak position, which indicates the degree of order of the monolayer (see also Figure 2). The different order in the SAMs was a consequence of the different substrate quality used to self-assemble the alkanethiols. Figure 6 clearly shows that as ν_a CH_2 shifts from 2920 to 2924 cm^{-1}; i.e., from SAM order to SAM disorder, the amount of electrically connected MB markedly increases. This result is in accordance with the conclusion drawn from the MB content vs n plot (Figure 5), indicating that highly ordered SAMs can not incorporate large quantities of MB because in this case there is a very limited number of defective regions allowing MB incorporation.

Incorporation is driven by concentration gradients and favored by the fact that MB is a highly lipophilic cation. For SAMs of short thiols (C ≤ C6) the process is reversible by simple changing the sign of the diffusion field (see Figure 4). On the other hand, for SAMs of longer thiols (C > C12) the small number of MB molecules that are incorporated into the SAM remain there, immobilized by van der Waals interactions and hydrophobic forces.

Interesting conclusions can be obtained by comparing the reductive desorption curves recorded for alkanethiol SAMs containing MB to those recorded for plain alkanethiol SAMs (Figure 7a). First, we obtain for all the SAMs, without and with MB, the same amount of charge ($q = 75 \pm 10\,\mu C\,cm^{-2}$) consistent with a dense standing up arrays of thiolates in $\sqrt{3} \times \sqrt{3}$ R30° or $c(4 \times 2)$ surface structure. This result suggests that no significant displacement of alkanethiol molecules by the MB species takes place. On the other hand, Figure 7b shows the desorption peak potential (Ep^D) as a function of n for freshly prepared alkanethiolate SAMs and alkanethiolate SAMs after MB incorporation. As already reported,[47,48] there is a linear relationship between the Ep^D and n up to C12. In this range as n is increased the Ep^D values shift to more negative potentials due to the increase in the attractive interaction between the chains, remaining almost constant for $n > 12$.[47] We observe a similar behavior for MB containing SAMs. However, while the slope is not changed (≈ 4 kJ mol^{-1} per C atom) there is a shift of Ep^D values to more negative potentials for short alkanethiols (Figure 7a,b). These data suggest that even small amounts of MB incorporated in short alkanethiols could stabilize the SAM structure against reductive desorption. Thus, more energy is needed to desorb the alkanethiol species from the Au surface (Figure 7a). On the other hand, no significant effect on Ep^D induced by MB incorporation was observed for the longer, more ordered alkanethiol SAMs (Figure 7b).The angle of the alkyl chains was determined for three representative SAMs (C6, C12, and C18) and MB-modified SAMs, as well.

(46) Flinkea, O. H. In *Electroanalytical Chemistry*; Bard, A. J., Rubinstein, I., Eds.; Marcel Dekker: New York, 1996; Vol. *19*.

(47) Kakiuchi, T.; Usui, H.; Hobara, D.; Yamamoto, M. *Langmuir* **2002**, *18*, 5231–5238.

(48) Vela, M. E.; Martin, H.; Vericat, C.; Andreasen, G.; Creus, A. H.; Salvarezza, R. C. *J. Phys. Chem. B* **2000**, *104*, 11878–11882.

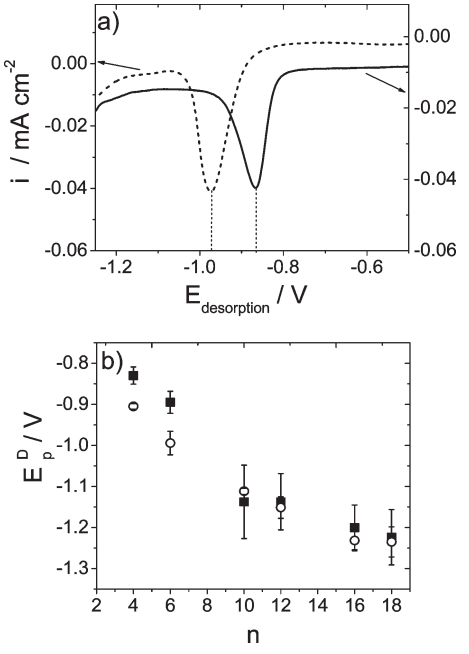

Figure 7. (a) Reductive desorption voltammperometry of C6 (—) and C6−MB (---) in 0.1 M NaOH. (b) Peak potential position (Ep^D) vs *n* from the reductive desorption voltammperometry (part a) for (■) alkanethiol self-assembled monolayers and (○) alkanethiol self-assembled monolayers containing MB.

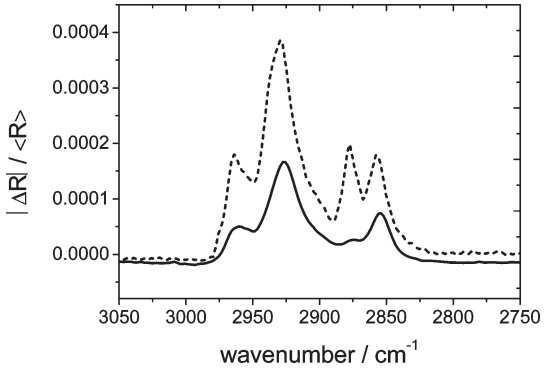

Figure 8. PMIRRAS spectra (3050−2750 cm^{-1} region) of a C6 SAM before (−) and after (---) immersion in 0.03 M aqueous MB solution for 24 h. Resolution was set to 4 cm^{-1} and 1500 scans were performed.

The spectra measured at 2900 cm^{-1} were fitted by gaussians. ν_a CH_3 and ν_s CH_2, being the more isolated peaks, were chosen to calculate the angles (see Figure 2). The maximum absorbance and peak areas were determined by using the 'relative' method (*vide infra*) in order to calculate the tilt angle. As expected,[37] an angle between 20° and 30° to the surface normal was found (C6, 31° ± 8; C12, 29° ± 4; C18, 30° ± 6). For SAMs of long alkanethiols the incorporation of MB brought no significant changes in these angles (C12/MB, 23° ± 13; C18/MB, 28° ± 8).

In contrast for C6 systems, a change in relative intensities for C6 and C6/MB is clearly seen (Figure 8). Two effects are noticeable. First, the increase in the intensity of CH_2 stretching vibrations that could be assigned to a change in the tilt angle of the hydrocarbon chains to less vertical with respect to metal surface. In fact, the dipole moment of the CH_2 stretching vibrations is perpendicular to the chain direction, and an increase in the signal should indicate an increase in the dipole moment interacting with the p-polarized light, i.e., a lead to the tilt angle increase. By using eq 1, we estimate an angle of 73° ± 5 for the C6 with incorporated MB (in contrast C6 31° ± 8). Second, there is a shift in the CH_2 asymmetric peak from 2929.0 to 2926.5 cm^{-1}. However, at present we do not have an explanation for these results, whose interpretation deserves more experimental work.

Conclusions

We have performed a detailed PMIRRAS, STM, and electrochemical study on the nonspecific interaction of MB molecules with alkanethiol self-assembled monolayers on Au(111). Results show that the amount of MB incorporated in the SAMs reaches a maximum for intermediate hydrocarbon chain lengths (C10−C12). We explain this behavior considering that SAMs of short alkanethiols (C ≤ C6), which are disordered, are able to incorporate large amounts of MB molecules but the interactions between the short chains and the MB molecules are not strong enough to efficiently retain the MB embedded in the SAM. On the other hand, SAMs of long alkanethiols (C > 12), which are ordered, have a small number of defective region so that incorporation of MB into the SAM is difficult. However, in this case the small number of incorporated molecules remains embedded in the SAM, immobilized by the hydrocarbon chain−MB interactions and hydrophobic forces. The role of chain disorder is demonstrated by preparing C12 SAMs of different quality: increasing SAM disorder results in more MB incorporation. This information is essential for design of efficient thiol-based Au vectors for transport and delivery of molecules as well as thiol-based Au devices for molecular sensing.

Acknowledgment. We acknowledge financial support from Nanotechnology Network PAE22711, ANPCyT (PICT06-621, PICT06-1146), and CONICET (PIP 112-200801-00362), Argentina. C.B. acknowledges the University of Buenos Aires for a financial support grant (UBACyT X-407). E.J.C., L.M.D.L., D.G., and R.C.S. are permanent fellows of CONICET. The present work was made in the frame of the CINN (INIFTA-INQUIMAE). V.Z. gratefully acknowledges the National Sciences and Engineering Research Council (NSERC) of Canada and the Canadian Foundation for Innovation (CFI) for financial assistance in a collaborative trip to Argentina.

Supporting Information Available: Figures showing the STM image of hexanethiol (C6) on Au(111) and text giving the analysis error for the PMIRRAS relative method used to calculate the angles of the SAMs. This material is available free of charge via the Internet at http://pubs.acs.org.